

# INFERRING EPIDEMICS FROM MULTIPLE DEPENDENT DATA VIA PSEUDO-MARGINAL METHODS

BY ALICE CORBELLA <sup>1,2,\*</sup>, ANNE M PRESANIS <sup>2,†</sup> PAUL J BIRRELL <sup>3,2,§</sup> AND DANIELA DE ANGELIS <sup>2,3,‡</sup>

<sup>1</sup>Department of Statistics, University of Warwick, \*alice.corbella@warwick.ac.uk

<sup>2</sup>MRC Biostatistics Unit, University of Cambridge, †anne.presanis@mrc-bsu.cam.ac.uk;  
‡daniela.deangelis@mrc-bsu.cam.ac.uk

<sup>3</sup>UK Health Security Agency §paul.birrell@phe.gov.uk

Health-policy planning requires evidence on the burden that epidemics place on healthcare systems. Multiple, often dependent, datasets provide a noisy and fragmented signal from the unobserved epidemic process including transmission and severity dynamics.

This paper explores important challenges to the use of state-space models for epidemic inference when multiple dependent datasets are analysed. We propose a new semi-stochastic model that exploits deterministic approximations for large-scale transmission dynamics while retaining stochasticity in the occurrence and reporting of relatively rare severe events. This model is suitable for many real-time situations including large seasonal epidemics and pandemics. Within this context, we develop algorithms to provide exact parameter inference and test them via simulation.

Finally, we apply our joint model and the proposed algorithm to several surveillance data on the 2017-18 influenza epidemic in England to reconstruct transmission dynamics and estimate the daily new influenza infections as well as severity indicators as the case-hospitalisation risk and the hospital-intensive care risk.

**1. Introduction.** State-space models (SSMs) have often been used to model the spread of a virus in a population, since they provide a practical and simple framework to describe the generation of epidemic time series (Dureau, Ballesteros and Bogich, 2013). SSMs are a latent variable representation of a dynamical systems evolving over specific domains (e.g. time, space, generations) (Schön et al., 2018). The definition of an SSM involves the specification of a system of stochastic or deterministic equations that define the behaviour of the latent process,  $X_t$ , where  $t$  indexes the domain (e.g. *time*), as well as the emission of observable quantities throughout the domain, denoted by  $Y_t$  (Birrell, De Angelis and Presanis, 2018). Thanks to their flexibility, SSM representations of observable phenomena have been widely used in many fields, from indoor positioning problems in engineering (Solin et al., 2018), to environmental studies (Anderson, 1996), to epidemic models (Magpantay et al., 2016).

Modelling epidemics as SSMs, the latent process generally encapsulates: (i) a transmission process, describing the spread of infection through a population, (ii) a severity process, modelling the likelihood of infected individuals to become severe cases (e.g. symptomatic, in need of hospitalization, etc.), and (iii) a detection process that links processes (i) and (ii) to available observations. Moreover, (iv) other sources of randomness might affect the generation of epidemic data, including seasonal fluctuations in parameters and misclassification of cases unrelated to the pathogen of interest.

---

*Keywords and phrases:* Epidemics, State-Space Models, Dependence, Pseudo-Marginal Methods, Evidence Synthesis, Data Fusion.

While formulating a SSM to describe epidemic data, there are several model choices to make; a key choice is the level of stochasticity of the overall system. As highlighted in the four points above, there are many possible sources of randomness, each of them could be accounted for in several different ways or could be overlooked through the use of deterministic systems, a reasonable approximation when numbers are sufficiently large. A model with a higher level of stochasticity attempts to make only few deterministic approximations and, the more the noise is ignored, the lower the level of stochasticity of the model.

Some models include complex dynamical components dynamic systems: [Birrell et al. \(2011\)](#), for example, assumes that an age-structured deterministic discrete-time system could approximate the spread of the 2009 pandemic influenza; it accounts for delays between infection and detection of symptomatic cases and places most of the randomness in the observation model. A similar approach, with even more complex layers, is considered in other works including [Weidemann et al. \(2014\)](#), analysing rotavirus data, and in recent works analysing COVID-19 data, e.g. [Keeling et al. \(2020\)](#) and [Birrell et al. \(2021\)](#). Conversely, other models adopt higher levels of stochasticity and rely on simplifying assumptions on the dynamics. An example is the work of [Lekone and Finkenstädt \(2006\)](#): here a discrete-time stochastic model is fitted to Ebola data and substantial, sometimes unrealistic, assumptions are made, including exponentially distributed time to events and full ascertainment of the cases. These kinds of models have been particularly utilised for small-size epidemics where the large-numbers deterministic approximation does not hold (e.g. [Nishiura \(2011\)](#), [Funk et al. \(2018\)](#)).

Hybrid models that exploit the strength from both approaches could potentially prove useful in many contexts. The transmission dynamics of large seasonal epidemics and of pandemics can be reliably approximated by deterministic systems, which, compared to their correspondent stochastic systems, allow greater model complexity (mixing heterogeneity, many compartments, etc.). In many contexts, however, the number of cases that become severe and detected might be smaller and subject to significant stochastic variation. Stochastic systems would be required to describe the severity process, marking a difference from many models listed above, where most of the randomness lies in the observational process.

While a model of this type (with all stochastic relationships except for the deterministic transmission dynamics) has greater realism, it might be more challenging under an inferential perspective, especially when multiple data sources are considered. If individuals are detected at different levels of severity in multiple datasets, an evidence synthesis framework ([Presanis et al., 2013, 2014](#)) should be employed, where correlations and delays among these layers of severity (and their related data sources) are accounted for.

This paper addresses the problem of inference of epidemics from multiple dependent data by presenting a general framework for the inferential problem; it identifies and tackles the challenges that arise in this context, considering the specific case of a deterministic-transmission model with multiple layers of stochasticity in the severity and detection stage. Section 2 provides a background to the methods used for modelling and inference, specifically SSMs and pseudo-marginal methods. Section 3 considers their application to the setting of epidemics, specifying a model that mirrors realistic situations; presents its problems and proposes an inferential routine. The aim of Section 4 is to compare the model presented in Section 3 to a similar model that, through a simplifying assumption does not account for the intrinsic dependence between datasets, inducing under-estimation of parameter uncertainty. Lastly Section 5 presents the analysis of real data on cases of seasonal influenza at different levels of severity, appropriately attributing stochasticity to each process.

**2. State-space models and their inference.** SSMs provide a flexible and general modelling framework for, among other problems, the inference of data arising from an epidemic. They are briefly outlined below, together with some useful tools to perform inference.

**2.1. Notation.** In this paper, Greek letters identify parameters (e.g.  $\theta, \lambda$ ) and their transformations ( $\xi = f(\theta)$ ). Parameters are random variables (r.v.s), here distinguished from the system's r.v.s, usually dependent on the parameters, denoted by uppercase Latin letters (e.g.  $X, Y$ ) and their instances which are lowercase ( $x, y$ ). Lower indexes indicate the domain (e.g.  $X_t$  is the r.v.  $X$  at time  $t$ ) and upper indices denote the states of the system ( $X^K, {}^J X^K$ ). Lastly, the notation  $1 : r$  is used to define a running index (e.g.  $y_{1:t}$  is the set of observation  $y_1, y_2, \dots, y_t$ ).

**2.2. State-space models.** A SSM is a stochastic process that makes use of a latent variable representation to describe dynamical phenomena (Schön et al., 2018). It has two components: a latent process,  $\{X_t\}_{t \geq 0}$  representing the underlying states and their dynamics; and an observed process  $\{Y_t\}_{t \geq 1}$ . Here, the domain of the process is assumed to be discrete time, with intervals indexed by  $t$ , although the methods reported are easily extended to other domains. A parameter-driven SSM can be defined through the state and the observation equations, as in Equations 1, 2 and 3, respectively

$$\begin{aligned} (1) \quad X_0 | \boldsymbol{\theta} &\sim p(x_0 | \boldsymbol{\theta}) \\ (2) \quad X_t | (X_{t-1}, \boldsymbol{\theta}) &\sim p(x_t | x_{t-1}, \boldsymbol{\theta}) \\ (3) \quad Y_t | (X_t, \boldsymbol{\theta}) &\sim p(y_t | x_t, \boldsymbol{\theta}) \end{aligned}$$

for  $t = 1, 2, \dots, T$ . These express the joint distribution of the initial state of the system,  $X_0$ , of the latent states,  $X_t$ s, and of the observations,  $Y_t$ s, parametrised by a vector  $\boldsymbol{\theta}$  (Brockwell et al., 2016). Equations 1 to 3 define a Markovian model. Markovianity is a common assumption for epidemic models and many other SSMs that fall in the category of partially observed Markov processes (POMPs) (King, Nguyen and Ionides, 2015) or hidden Markov models (HMMs) (Churchill, 2005).

A Markovian SSM defines the following full probability model:

$$(4) \quad p(x_{0:T}, y_{1:T} | \boldsymbol{\theta}) = \prod_{t=1}^T p(y_t | x_t, \boldsymbol{\theta}) \prod_{t=1}^T p(x_t | x_{t-1}, \boldsymbol{\theta}) p(x_0 | \boldsymbol{\theta})$$

where, thanks to Markovianity and conditional independence, the joint density can be factorised into the state and observation densities.

A SSM can also be represented through a graphical model where a graph  $\mathcal{G} = (\mathcal{V}, \mathcal{E})$  represents the conditional independence structure (edges  $\mathcal{E}$ ) between r.v.s (nodes  $\mathcal{V}$ ). Some graphical models representing the state and observational process of an SSM are illustrated in Figure 1; the dependence on the parameter  $\boldsymbol{\theta}$  is omitted for simplicity.

This framework could account for many different modelling assumptions, including multidimensional state processes or deterministic relations, as exemplified in Figure 1.

**2.3. Inference in state-space models.** Observations  $\{Y_t\}_{t \geq 1}$  can be used to infer the state process  $\{X_t\}_{t \geq 0}$ , usually conditional on specific values of the static parameter  $\boldsymbol{\theta}$ , or to estimate the static parameter  $\boldsymbol{\theta}$ , usually marginally on the distribution of the state process.

**2.3.1. State inference.** State inference could have multiple perspectives, for a full review of these see Lindsten and Schön (2013); in this paper the inference relies on the estimation of the filtering distribution,  $p(x_t | y_{1:t}, \boldsymbol{\theta})$ , for  $t = 1, \dots, T$ , which is the state distribution at time  $t$ , conditional on the data and parameters.

The filtering distribution, except for few cases (e.g. linear Gaussian SSMs (Kalman, 1960)), can be approximated recursively by a two-step procedure that alternates approximation of the state distribution given the observations (measurement update) and given the previous states (prediction update).

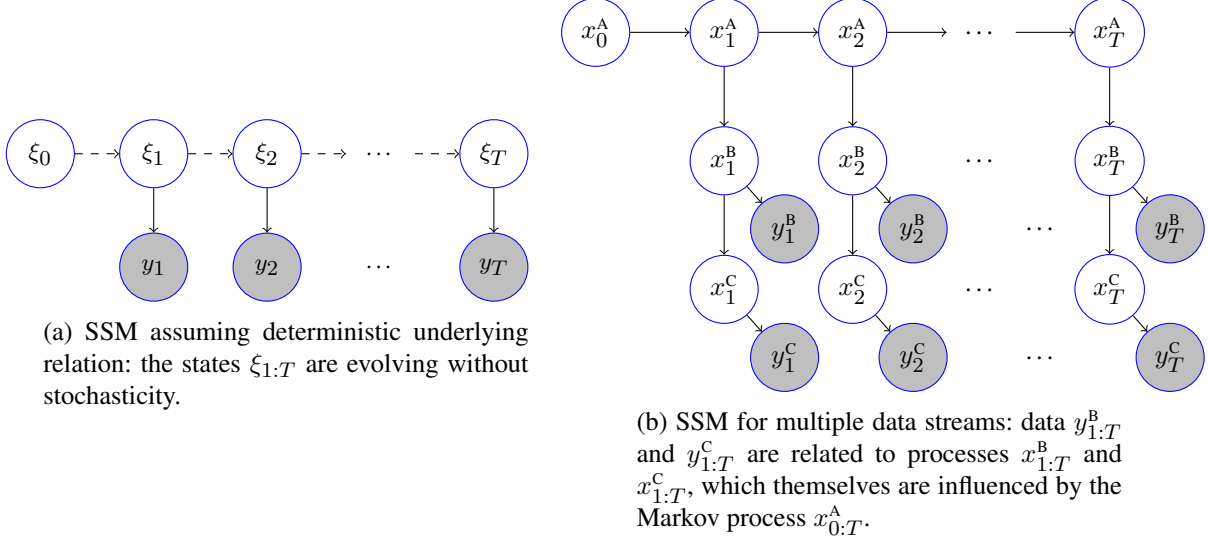


Fig 1: Some examples of graphical models for SSMs. Grey nodes correspond to observed variables and white nodes are latent variables. Solid arrows express stochastic dependence among r.v.s, while dashed arrows express deterministic links.

The sequential simulation of samples from the distributions  $X_t|y_{1:t}, \theta$  and  $X_t|y_{1:t-1}, \theta$  allows the approximation of the likelihood of the data  $y_{1:T}$ , given a parameter value  $\theta$  and marginally w.r.t. the state distribution  $X_{1:T}$  in Equation 5:

$$(5) \quad p(y_{1:T}|\theta) = \prod_{t=1}^T p(y_t|y_{1:t-1}, \theta) = \prod_{t=1}^T \int_{X_{0:t}} p(y_t, x_{0:t}|y_{1:t-1}, \theta) dx_{0:t}$$

The most common among these simulation-based procedures is the bootstrap particle filter (BPF) (Arulampalam et al., 2002), which uses the state and observation equations to iterative propose and weight samples to approximate the filtering distribution. The BPF provides an unbiased estimator  $\hat{p}(y_{1:T}|\theta)$  of the likelihood of the data given a parameter value  $\theta$  which can be used to perform inference.

A full derivation of Equation 5 and of the BPF is not necessary for the understanding of this paper, we leave curious readers to consult Chapter 4 of Corbella (2019) and Lindsten and Schön (2017).

**2.3.2. Parameter inference.** There is not a unique way in which this approximated likelihood can be used to drive inference on the parameter  $\theta$ . Within the Bayesian framework, assumed here to enable a complex synthesis of available evidence, many iterative algorithms have been developed to sample from the posterior distribution of interest,  $\Theta|y_{1:t}$ , when only an approximation of the likelihood is available. Andrieu, Doucet and Holenstein (2010) review and summarise the algorithms used more frequently for parameter inference in SSMs. Among the algorithms listed, pseudo-marginal approaches, previously introduced in Andrieu and Roberts (2009), provide a simple way to integrate simulation-based approximation of the likelihood (such as the BPF) into Monte Carlo Markov chain (MCMC) algorithms for Bayesian inference.

Pseudo-marginal algorithms are aimed at exploring only the posterior distribution of the parameter, marginally from the distribution of the states, and they are based on the classical Metropolis Hastings (MH) algorithm (Metropolis et al., 1953; Hastings, 1970). Differently

from the original MH algorithm, here the unnormalised posterior distribution is approximated by the product of the prior and a simulation-based approximation of the likelihood in the acceptance ratio (e.g. the BPF). Two pseudo-marginal algorithms are employed throughout this paper: grouped independence Metropolis Hastings (GIMH) (Beaumont, 2003) and Monte Carlo within Metropolis (MCWM) (Andrieu and Roberts, 2009).

**2.4. State-space models for epidemics.** The SSM methodology marries well with epidemic models: available data are only a partially-observed signal of latent variables which encapsulate all the processes involved in the data generation (e.g. transmission, severity, background noise). More specifically, transmission models usually consists of stochastic or deterministic systems of equations that describe the flow of individuals between disjoint compartments according to their disease status: susceptible, infectious, recovered and immune, etc.

Even the first epidemic models formulated (Kermack and McKendrick, 1927) could be seen from a SSM perspective: the state system describes the deterministic transmission dynamics via differential equations and the observational process consists of the detection likelihood. This approach has endured over time: the deterministic transmission dynamics enable the modelling of several complex aspects of an epidemic (e.g. heterogeneous populations, non-exponential transition time, see Keeling and Rohani (2011)) and, when large populations are considered, they approximate well the correspondent stochastic system (Diekmann, Heesterbeek and Britton, 2012). However this kind of model relies on the unrealistic assumption that the only source of noise observed in the data is caused by the case ascertainment/detection randomness.

Another stream of literature models explicitly the transitions among disease status as random variables, assuming a stochastic state process. Before the advent of simulation-based inference for SSMs, the inference for these models heavily relied on simplifying model assumptions to derive closed forms of the likelihood (Britton, 2010; Andersson and Britton, 2012).

Finally in recent decades, SSM methodology has been used for epidemic dynamics more explicitly. Some notable works include Bretó et al. (2009); Dukic, Lopes and Polson (2012); Dureau, Ballesteros and Bogich (2013); McKinley et al. (2014); Shubin et al. (2016). Even if, as illustrated in Section 2.3, SSM inference is possible (both with pseudo-marginal methods and other algorithms), many simplifying assumptions are needed to allow computation under time constraints. These simplifications often include assuming independence between data stream, dropping transmission compartments, assuming full ascertainment of the cases, and discretizing time in large intervals. Moreover, some but not all parts of the state process of these models involve large numbers, and could be reliably approximated by its deterministic counterpart.

Within the application of SSMs to epidemics, there seem to be a lack of hybrid models that exploits the deterministic approximations of transmission dynamics that characterise large epidemics and pandemics while proper accounting for stochasticity in the latent states that cannot be approximated, e.g. the states that involve severe cases. In the remainder of the paper we will propose and discuss such a semi-stochastic model, with a particular focus on its use when multiple *dependent* data are available.

**3. Multiple data on epidemics.** When a virus spreads in a population, multiple signals of its presence could be available in the form of time-series counts. Each of these counts is likely to be related to a specific level of severity (e.g. mild symptomatic cases, patients that require hospitalization) and could be affected by specific sources of noise and, possibly bias. Nevertheless, all data are linked to the underlying system that describes the transmission process in the population. Therefore, the joint analysis of multiple data allows better knowledge than separate analyses of single datasets, but introduces several challenges.

3.1. *Dependency between data streams at time  $t$ .* Let  $X_t^0$  be the process describing the number of new infections at time  $t$  of a specific epidemic in a given population. Infected individuals could experience a series of increasingly severe events in a pyramid perspective (Presanis et al., 2009), e.g. they might experience mild symptoms, be hospitalised, require intensive care, die; with cases in each severity layer being a subset of the cases in the previous layer as represented in Figure 2a. The process describing the number of individuals experiencing an event  $J$  among these severity layers is denoted by  $X_t^J$ , experiencing event  $K$  by  $X_t^K$ , etc. for  $t = 1, \dots, T$ , with  $J = 0$  representing infection.

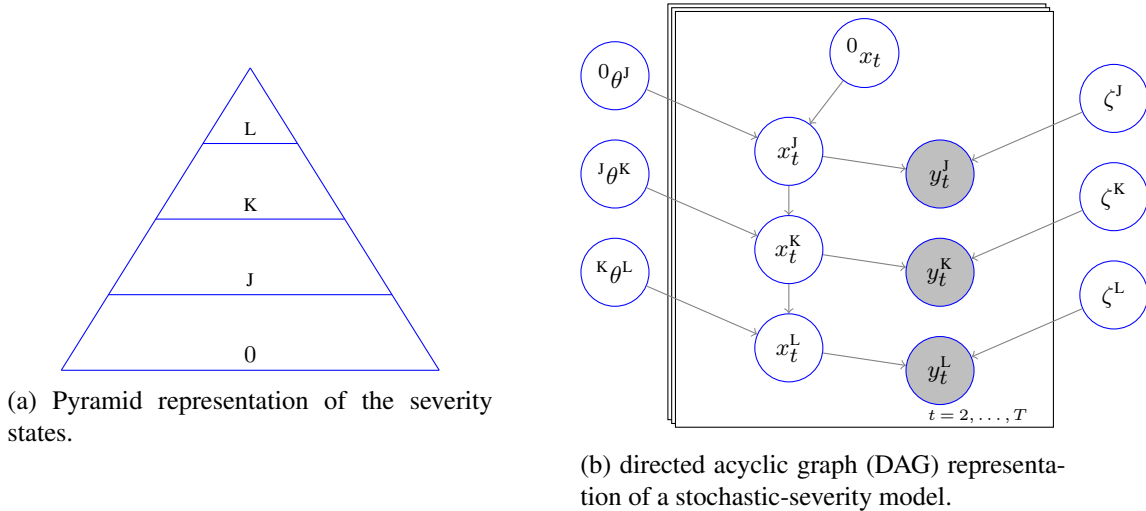


Fig 2: Pyramid representation and DAG of a severity process.

A simple model would assume that the number of people in a severity category would be a subsample (e.g. a Binomial sample) of the number of people in the less-severe category with severity parameters  ${}^J\theta^K$  encapsulating the risk of moving from severity state  $J$  to  $K$ . The observational processes would describe the number of detected cases in each specific severity layer  $Y_{1:t}^J$ , as, again a subsample of the cases in a specific layer  $J$  with a layer-specific detection probability  $\zeta^J$ . Figure 2b illustrates a model of this type comprising 3 events of increasing severity and the connection among multiple data can be easily spotted: i.e. not only they are linked through the underlying infection process, but also via the progression through severity states. In fact, while distributional properties could be used to write the likelihood of each of multiple datasets given the infection process  $X_{1:t}^0$  and some parameters, these data are not independent, conditionally on the parameters: they share common severity processes  $X^J, X^K, X^L$ , and therefore cannot be simply multiplied to obtain a joint likelihood of the data.

3.1.1. *Dependency between data streams across time.* Another challenge is given by delays between events: severe events usually do not happen simultaneously. More likely, there will be some time elapsing between events of increasing severity; this could lead to, for example, cases detected in severity layer  $J$  at time  $t$ , be present in data on layer  $K$  at some time  $t + s, s \geq 0$  with some chance. This introduces dependence not only between observations at different levels of severity at the same time, but also across time.

To include delays, a new notation is introduced: denote by  ${}^t X^K$  the number of people that will eventually experience severe event  $K$ , having already experienced event  $J$  at  $t$ ; and by

${}^J_t X_s^K$  the number of people that experience event K at time  $s$ , having already experienced event J at  $t$ . Thus, the subscript and superscript on the right side denote the time and type of final events and the ones on the left side denote the time and type of a previous event. When only the right superscript/subscript is reported, e.g.  $X_t^K$ , as in the previous section, this denotes the number of people experiencing event K at  $t$  irrespectively from the time of previous event, which can be obtained summing over the number of people experiencing event  $j$  at the previous event times:  $X_s^K = \sum_{t \leq s} {}^J_t X_s^K$ .

A stochastic model for the time series  ${}^J_{1:T} X^K$  of the number of people that have had event J at time  $t$  ( $t = 1, \dots, T$ ) and will experience event K can be specified by, for example, a Binomial sample:

$$(6) \quad ({}^J_t X^K | x_t^J) \sim \text{Bin}(x_t^J, {}^J \theta^K)$$

for  $t = 1, \dots, T$ . Denote by  ${}^J f_d^K({}^J \vartheta^K)$  the probability that the delay experienced between event J and K is in the  $d$ th interval of length  $\delta$ ,  $[\delta d; \delta d + \delta)$  for  $d = 0, 1, \dots, D$ , with  $D$  being the largest interval index for which the delay is relevant (i.e.  ${}^J f_d^K({}^J \vartheta^K) \approx 0$  for  $d > D$ ).  ${}^J f_d^K({}^J \vartheta^K)$  is often derived from the discretization of a parametric distribution with appropriate parameter vector  ${}^J \vartheta^K$ . To make the notation lighter,  ${}^J \vartheta^K$  is dropped, with  ${}^J f_d^K$  representing both the function and the parameters used to describe the delay from J to K.

Under this discrete definition of the distribution of the time to event, and conditionally on  ${}^J_t X^K$ , the introduction of stochastic delays could be allowed by defining  ${}^J_t X_s^K$ , as a component of the Multinomial r.v.:

$$(7) \quad {}^J_{t:t+D} X^K | {}^J_t x^K \sim \text{Multi}({}^J_t x^K, {}^J f_{0:D}^K).$$

with  ${}^J f_{0:D}^K = ({}^J f_0^K, {}^J f_1^K, \dots, {}^J f_D^K)$  the vector containing the probabilities for the waiting time between 0 and J as described above. The number of people that experience event K at each time  $t = 1, \dots, T$  can then be obtained by summing these stochastic terms, i.e.:

$$(8) \quad X_t^K = \sum_{d=0}^D {}^J_{t-d} X_t^K,$$

which can be recognised as a typical stochastic convolution to describe delays in epidemic models (Brookmeyer et al., 1994). The counts of events at a higher level of severity can be modelled likewise.

This form of delay structure, as many other stochastic delay formulations, introduces a dependence over time. This is evident in Equation 7, where the number of people experiencing K at time  $t$  depends on r.v.s defined on the previous  $D$  intervals.

**3.2. A model for multiple data on severe influenza.** Influenza is monitored by many surveillance schemes in the UK, one of these is the Severe Acute Respiratory Infection (SARI)-Watch scheme (UK Health Security Agency (UKHSA), 2021), which has evolved from the UK Severe Influenza Surveillance System (USISS), the main source of data on severe influenza cases in the UK prior to the COVID-19 pandemic. According to the USISS protocol (Health Protection Agency, 2011a), all National Health Service (NHS) trusts in England report, among other things, the weekly number of laboratory-confirmed influenza cases admitted to Intensive Care (IC) units. In addition to this mandatory scheme, a sentinel subgroup of NHS trusts in England is recruited every year to participate in the USISS sentinel scheme (Health Protection Agency, 2011b; Boddington, Verlander and Pebody, 2017), which reports weekly numbers of laboratory-confirmed influenza cases hospitalised at all levels of care. Some individuals might be detected in both datasets, leading to a dependence.

3.2.1. *Parametrization and data generation.* Denote by  $\theta$  the set of parameters, composed of  $\theta^T$ , the parameters of a *SEIR* transmission model, tracking the number of susceptible ( $S$ ), exposed ( $E$ ), infected ( $I$ ) and removed ( $R$ ), individuals, and  $\theta^S$ , the parameters of the severity and detection model.

$\theta^T = \{\pi, \iota, \sigma, \gamma, \beta\}$  consists of the transmission rate  $\beta$ ; the exit rates from compartments  $E$  and  $I$ ,  $\sigma$  and  $\gamma$  respectively; and the initial proportions immune,  $\pi$ , and of infected/infectious,  $\iota$ . The parameters  $\pi$  and  $\iota$ , together with  $\sigma$ ,  $\gamma$  and the known constant  $N$ , the total size of the population, contribute to the formulation of the initial state of the epidemic. Seasonal influenza is a large epidemic that takes place every winter with high likelihood, hence a deterministic transmission model is assumed: the information contained in  $\theta^T$ , together with the known constants, provides the full time series of the number of new infections. Let the time be discretised in intervals of length  $\delta$  so that the  $t$ -th interval covers the time  $[t\delta, t\delta + \delta)$  and the intervals are indexed by  $t = 0, 1, 2, \dots, T$ , where  $t = 0$  coincides with the beginning of the data collection period and  $t = T$  is the end of the data collection period. Denote the number of susceptible individuals at the beginning of interval  $t$  by  $S_t$  and likewise for the other compartments  $E, I, R$ . Denote by  $\xi_{1:T}^0$  the vector of the number of new infections in interval  $t = 0, 1, 2, \dots, T$ .

$\theta^S = \{{}^0\theta^H, {}^H\theta^{IC}, {}^0f^H, {}^Hf^{IC}, \zeta_t^H, \zeta_t^{IC}\}$  includes severity and detection parameters:  ${}^0\theta^H$  is the probability of hospitalization given infection;  ${}^H\theta^{IC}$  is the probability of IC admission given hospitalization;  ${}^0f^H$  and  ${}^Hf^{IC}$  denote probabilities for the times from infection to hospitalisation and from hospital admission to IC admission, respectively;  $\zeta_t^H$  and  $\zeta_t^{IC}$  are the probability of detecting an hospitalised and IC case, respectively.

The transmission and severity compartments are reported in Figure 3.

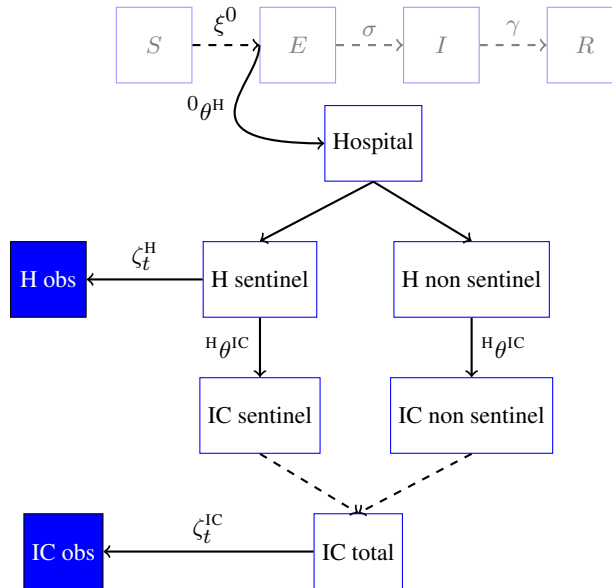


Fig 3: Flowchart of the possible severe events recorded in USISS.

3.2.2. *SSM formulation.* Describing the model using SSM notation, the state process is composed of the distributions of:  ${}_t^0X^H$ , the number of hospitalizations that were infected at each interval  $t$ ;  $X_t^H$ , the number of hospitalizations at  $t$ , obtained via a convolution of  ${}_t^0X^H$ ; the number of hospitalizations that eventually will be admitted to IC and have been

hospitalised at  $t$ ,  ${}^H X_t^{\text{IC}}$ ; the number of IC admissions at  $t$ ,  $X_t^{\text{IC}}$  obtained by the convolution of  ${}^H X_t^{\text{IC}}$ , for  $t = 0, 1, 2, \dots, T$ . The state process is described as:

$$\begin{aligned}
 (9) \quad & \left( {}^0 X_t^{\text{H}} \right) \sim \text{Pois}({}^0 \xi \cdot {}^0 \theta^{\text{H}}) \\
 & \left( {}^0 X_{t:t+D}^{\text{H}} \mid {}^0 X_t^{\text{H}} = {}^0 x_t^{\text{H}} \right) \sim \text{Multi}({}^0 x_t^{\text{H}}, {}^0 f_{0:D}^{\text{H}}), \quad X_t^{\text{H}} = \sum_{s=0}^S {}^0 X_{t-s}^{\text{H}} \\
 & \left( {}^H X_{t:t+D}^{\text{IC}} \mid {}^H X_t^{\text{IC}} = {}^H x_t^{\text{IC}} \right) \sim \text{Multi}({}^H x_t^{\text{IC}}, {}^H f_{0:D}^{\text{IC}}), \quad X_t^{\text{IC}} = \sum_{s=0}^S {}^H X_{t-s}^{\text{IC}}
 \end{aligned}$$

for  $t = 0, 1, \dots, T$ . Here  ${}^0 f_{0:D}^{\text{H}}$  and  ${}^H f_{0:D}^{\text{IC}}$  are vectors containing elements  ${}^0 f_d^{\text{H}}$  and  ${}^H f_d^{\text{IC}}$  denoting the probability of experiencing a delay of  $d$  weeks between infection and hospitalization and hospitalization and IC admission, respectively, for  $d = 0, \dots, D$ . These are considered known and fixed.

The observational process, consists of the distributions of two datasets,  $y_{1:T}^{\text{H}}$ , the count of hospitalizations, and  $y_{1:T}^{\text{IC}}$ , the count of IC admissions, conditional on the hidden states  $X_{1:T}^{\text{H}}$  and  $X_{1:T}^{\text{IC}}$ . These are assumed to be Binomial with detection probabilities  $\zeta_t^{\text{H}}$  and  $\zeta_t^{\text{IC}}$  respectively:

$$(10) \quad \begin{aligned} (Y_t^{\text{H}} \mid X_t^{\text{H}} = x_t^{\text{H}}) & \sim \text{Bin}(x_t^{\text{H}}, \zeta_t^{\text{H}}) \\ (Y_t^{\text{IC}} \mid X_t^{\text{IC}} = x_t^{\text{IC}}) & \sim \text{Bin}(x_t^{\text{IC}}, \zeta_t^{\text{IC}}) \end{aligned}$$

for  $t = 0, 1, 2, \dots, T$ .

**3.3. Inference.** Two inferential methods are proposed here: the first does not account for the dependence among data while the second properly encapsulates the layers of stochasticity present in the model.

**3.3.1. The approximation under an independence assumption.** Thanks to the Poisson properties (Kingman, 1992), several hidden states and the data distribute marginally according to a Poisson distribution:

$$\begin{aligned}
 (11) \quad & X_t^{\text{H}} \sim \text{Pois} \left( {}^0 \theta^{\text{H}} \cdot \sum_{d=0}^D {}^0 \xi_{t-d}^0 \cdot {}^0 f_d^{\text{H}} \right) \\
 & X_t^{\text{IC}} \sim \text{Pois} \left( {}^H \theta^{\text{IC}} \cdot {}^0 \theta^{\text{H}} \cdot \sum_{d=0}^D \sum_{g=0}^d {}^0 \xi_{t-d}^0 \cdot {}^0 f_d^{\text{H}} \cdot {}^H f_g^{\text{IC}} \right) \\
 & Y_t^{\text{H}} \sim \text{Pois} \left( \zeta_t^{\text{H}} \cdot {}^0 \theta^{\text{H}} \cdot \sum_{d=0}^D {}^0 \xi_{t-d}^0 \cdot {}^0 f_d^{\text{H}} \right) \\
 & Y_t^{\text{IC}} \sim \text{Pois} \left( \zeta_t^{\text{IC}} \cdot {}^H \theta^{\text{IC}} \cdot {}^0 \theta^{\text{H}} \cdot \sum_{d=0}^D \sum_{g=0}^d {}^0 \xi_{t-d-g}^0 \cdot {}^0 f_d^{\text{H}} \cdot {}^H f_g^{\text{IC}} \right)
 \end{aligned}$$

for  $t = 0, 1, 2, \dots, T$ .

Ignoring the dependence between the two data streams, the joint likelihood is

$$(12) \quad p(y_{1:T}^{\text{H}} \mid \xi_{1:T}^0, {}^0 \theta^{\text{H}}, \zeta_{1:T}^{\text{H}}) \times p(y_{1:T}^{\text{IC}} \mid \xi_{1:T}^0, {}^H \theta^{\text{IC}}, {}^0 \theta^{\text{H}}, \zeta_{1:T}^{\text{IC}}),$$

where each factor is the Poisson density of Equation 11.

The independence assumption would substantially simplify inference since, with a likelihood available in closed form, there would be no need of a simulation-based estimation of the likelihood and, indeed, of pseudo-marginal methods. The aim of Section 4 is to assess if this approximation induces any error in terms of bias or uncertainty quantification.

**3.3.2. Exact inference via pseudo-marginal methods.** To properly account for dependence and stochasticity, a simulation algorithm is proposed to approximate the joint likelihood of the hospitalization and IC data. The joint probability distribution can be decomposed in two ways:

$$\begin{aligned} p(y_{1:T}^H, y_{1:T}^{IC} | \boldsymbol{\theta}) &= p(y_{1:T}^H | y_{1:T}^{IC}, \boldsymbol{\theta}) p(y_{1:T}^{IC} | \boldsymbol{\theta}) \\ &= p(y_{1:T}^{IC} | y_{1:T}^H, \boldsymbol{\theta}) p(y_{1:T}^H | \boldsymbol{\theta}) \end{aligned}$$

where, in both cases, the second of the two factors is available in closed form (Equation 11).

To approach the estimation of the other factor, state-inference methods for SSMs can be used. The methods for inference described in Section 2 address the Markovian dependence across time. Here however, the time-dependence of the transmission process disappears thanks to the deterministic approximation. However, the dependence over the severity domain remains: the distributional assumptions of Equation 9 can be used to construct a simulation-based estimator of the likelihood that sequentially approximates severity states.

Algorithm 1 exploits the first decomposition, where  $p(y_{1:T}^{IC} | \boldsymbol{\theta})$  is available in closed form and a solution is needed for  $p(y_{1:T}^H | y_{1:T}^{IC}, \boldsymbol{\theta})$ , which is obtained by approximating the  $T$ -dimensional integral:

$$\begin{aligned} p(y_{1:T}^H | y_{1:T}^{IC}, \boldsymbol{\theta}) &= \int_{X_1^H} \dots \int_{X_T^H} p(y_{1:T}^H, X_{1:T}^H | y_{1:T}^{IC}, \boldsymbol{\theta}) dX_1^H \dots dX_T^H \\ &= \int_{X_1^H} \dots \int_{X_T^H} p(y_{1:T}^H | X_{1:T}^H, y_{1:T}^{IC}, \boldsymbol{\theta}) p(X_{1:T}^H | y_{1:T}^{IC}, \boldsymbol{\theta}) dX_1^H \dots dX_T^H \\ &= \int_{X_1^H} \dots \int_{X_T^H} p(y_{1:T}^H | X_{1:T}^H, \boldsymbol{\theta}) p(X_{1:T}^H | y_{1:T}^{IC}, \boldsymbol{\theta}) dX_1^H \dots dX_T^H \end{aligned}$$

The simulation of the hidden states is made simple by the distribution chosen for the severity and detection process.

A second algorithm uses the alternative factorization of the joint likelihood. While still feasible, this algorithm performs more poorly than Algorithm 1, mainly because the IC admissions are more-completely observed and smaller in numbers, hence particle degradation is more likely to take place (Brooks et al., 2011). See the Supplementary information for the derivation of the two algorithms.

**4. Relevance of the dependence.** A full simulation study is set up to assess whether (and in which situations) accounting for the dependence makes any difference compared to assuming the two datasets to be independent. Intuitively, a miss-specified model that does not account for dependencies would assume more independent information than is truly present in the dependent data, hence would achieve overly-confident results. Conversely, truly accounting for dependence should reflect more properly the unknowns and noise of the model and also help the estimation of those parameters that effectively link the dependent data streams.

**Result:**  $\hat{p}(y_{1:T}^H, y_{1:T}^{IC} | \theta)$

**Input:** fixed parameter  $\theta$ , number of particles  $N$ , data  $y_{1:T}^H, y_{1:T}^{IC}$

compute

$p(y_{1:T}^{IC} | \theta) = f(y_{1:T}^{IC} | \zeta_t^H \cdot {}^H\theta^{IC} \cdot {}^0\theta^H \cdot \sum_{d=0}^D \sum_{g=0}^d \xi_{t-d-g}^0 \cdot {}^0f_d^H \cdot {}^Hf_g^{IC})$  with  $f(\cdot)$  being a Poisson density

**for**  $n = 1, \dots, N$  **do**

**for**  $t = 0, 1, \dots, T$  **do**

        sample :  $x_t^{IC(n)} \sim \text{Pois} \left( (1 - \zeta_t^H) [{}^H\theta^{IC} \cdot {}^0\theta^H \sum_{d=0}^D \sum_{g=0}^d \xi_{t-d-g}^0 \cdot {}^0f_d^H \cdot {}^Hf_g^{IC}] \right) + y_T^{IC}$

        sample :  ${}^Hx_{t-1}^{IC(n)}, \dots, {}^Hx_S^{IC(n)} \sim \text{Multi} \left( x_t^{IC(n)}, {}^Hf_{1:S}^{IC} \right)$

        compute :  ${}^Hx_t^{IC(n)} = \sum_{s=1}^S {}^Hx_s^{IC(n)}$

        sample :  $x_t^H | {}^Hx_t^{IC(n)}, \theta \sim \text{Pois} \left( (1 - {}^H\theta^{IC}) \left[ {}^0\theta^H \sum_{d=0}^D \xi_{t-d}^0 \cdot {}^0f_d^H \right] \right) + {}^Hx_t^{IC(n)}$

**end**

    compute :  $p(y_{1:T}^H | {}^Hx_{1:T}^H, \theta) = g \left( y_{1:T}^H | {}^Hx_{1:T}^H, \zeta_t^H \right)$  with  $g(\cdot)$  being a Binomial density

**end**

$\hat{p}(y_{1:T}^H, y_{1:T}^{IC} | \theta) = p(y_{1:T}^{IC} | \theta) \cdot \frac{1}{N} \sum_{n=1}^N p(y_{1:T}^H | {}^Hx_{1:T}^H, \theta)$

**Algorithm 1:** Approximation of the likelihood  $p(y_{1:T}^H, y_{1:T}^{IC} | \theta)$

4.1. *Simulation study set-up.* The simulated data are formulated to reflect a situation similar to the motivating USISS data on a smaller population, chosen to reduce the computation time. The datasets are generated with some common parameters and some scenario-specific parameters.

The common parameters are:

$$\left\{ N = 10000, \beta = 0.63, \pi = 0.3, \iota = 0.0001, \sigma = \frac{1}{4}, \gamma = \frac{1}{3.5}, {}^0f^H \sim \text{Exp}(0.3), {}^Hf^{IC} \sim \text{Exp}(0.4) \right\}$$

while the scenario specific parameters are reported in Table 1. Each of the severity and detection parameters can take either a small or a large value. The smaller leads to situations where the probability of being observed in both datasets is low, therefore data are less dependent; while when parameters take larger values, there is more overlap between datasets and therefore more dependence. The values have been chosen to be at the extremes of a realistic range:

TABLE 1  
Parameters used to generate the datasets.

	small dependence	large dependence
${}^0\theta^H$	0.1	0.5
${}^H\theta^{IC}$	0.1	0.9
$\zeta_t^H = \zeta^H$	0.1	0.3
$\zeta_t^{IC} = \zeta^{IC}$	0.1	0.9

e.g., the probability of hospitalization and the detection of hospitalization in the large dependence case are smaller than the respective quantities for IC unit admission because usually more severe cases are better monitored, and hence have a higher detection.

The aim of the comparison is to assess whether a misspecified independent likelihood (Equation 10) would affect the inference of the parameters, leading to different posterior distributions from the ones obtained with the Monte Carlo (MC) approximation of the joint likelihood assuming dependent data (Algorithm 1). For this reason the results presented here

are to be compared within each scenario: between the ones obtained with the independent misspecified model (abbreviated with MISS IND) and the ones obtained using the dependent joint model (abbreviated with JOINT DEP).

**4.2. Results of the simulation study.** As outlined in detail below, the misspecified model leads to overly precise results in the estimation of the transmission parameters when the dependence is large. Furthermore, the parameter connecting the two severity states to which the data refer is estimated with less precision when the misspecified model is assumed.

**4.2.1. Comparison for transmission parameters.** For the parameter inference with the approximated joint likelihood, a MCWM algorithm with likelihood approximation via Algorithm 1 with  $N = 2000$  was chosen. Resulting estimates were compared with those from the misspecified independent Poisson likelihood over 1000 synthetic datasets. 500 datasets were simulated using the smaller values of the parameters (left column of Table 1) and 500 datasets using the larger values (right column of Table 1). The only parameters inferred are the transmission parameters  $\beta, \iota$  and  $\pi$ , with the severity parameters being fixed at their true, scenario-specific, value.

In the case of small dependence, the results show that the posterior distributions obtained with the misspecified independent likelihood are very similar to the ones obtained with the approximated joint likelihood. To measure any discrepancy between the two estimation methods, the pairwise difference (PWD) in variance  $\text{Var}(\hat{\alpha}^m | y^d)$  for  $m \in \{\text{JOINT DEP, MISS IND}\}$  and  $\alpha$  being one of the parameters, and in the width  $R_{95}(\hat{\alpha}^m | y^d)$  of the 95% Credible Intervals (CrIs) was computed as:

$$\begin{aligned} \text{PWD}(\text{Var}(\alpha))^d &= \text{Var}(\hat{\alpha}^{\text{JOINT DEP}} | y^d) - \text{Var}(\hat{\alpha}^{\text{MISS IND}} | y^d) & \alpha = \beta, \pi, \dots; d = 1, 2, \dots, 500 \\ \text{PWD}(R_{95}(\alpha))^d &= R_{95}(\hat{\alpha}^{\text{JOINT DEP}} | y^d) - R_{95}(\hat{\alpha}^{\text{MISS IND}} | y^d) & \alpha = \beta, \pi, \dots; d = 1, 2, \dots, 500. \end{aligned}$$

These quantities are reported in Figure 4 (top) which shows an imperceptible difference in the posterior distributions and their precision-summaries between the two models.

The same analysis is run on the 500 datasets with a large dependence, with results reported in Figure 4 (bottom). Here there is a notable difference between the results from the two models: the posterior distributions from the misspecified model that assumes independent data are less variable than the ones derived using the MC approximation of the joint dependent likelihood.

This result was expected, since the misspecified model, by assuming independent data, accounts for more information than is contained in the data. This leads to an overconfidence that can be detected in the underestimation of the posterior variance. Results are confirmed by the proportion of datasets for which the pairwise differences are less than or equal to 0 for each of the parameters (Table 2). When this quantity is close to 0.5, the variances of the estimates obtained with the two methods are similar within datasets; when this quantity is close to 1 it suggests that the variance of the estimates obtained using the misspecified independent likelihood is systematically larger than the variance of the estimates obtained with the joint likelihood; and when this quantity is close to 0 it highlights that the former variance is systematically smaller than the latter. The results strongly suggest a systematic difference in variability between the two methods in the large dependence scenario. In all the simulated datasets the variances of the posterior distributions of the parameters are smaller in the analysis using the misspecified independent model than in the approximate joint model.

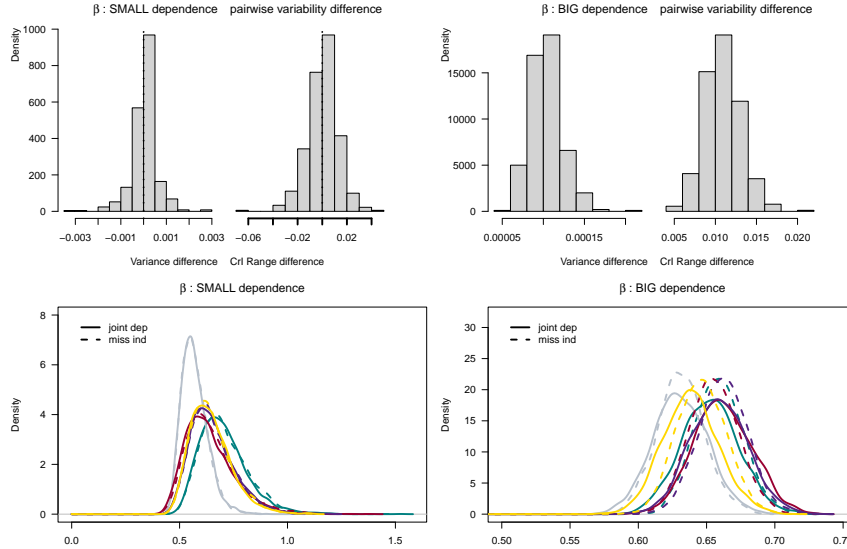


Fig 4: Histogram of the pairwise differences in variance and in 95% Credible Interval (Crl) length of the posterior distribution of the transmission parameters  $\beta$  for the small dependence scenario (left) and big dependence scenario (right). The bottom plots report the posterior distribution estimated with the JOINT DEP (solid) and MISS IND (dashed) model for 5 randomly-selected simulated data (colors).

TABLE 2  
*Proportion of datasets in which the pairwise difference of variance is smaller or equal to 0 for the three transmission parameters.*

Parameter	Proportion of PWD(Var) $\leq 0$	
	Small dependence	Large dependence
$\beta$	0.392	0
$\pi$	0.390	0
$\iota$	0.378	0

4.2.2. *Comparison for transmission and severity parameters.* The same comparison is carried out in a context where inference is drawn both for the transmission and the severity parameters. Here, since more quantities are estimated and due to the high correlation of the parameters of epidemic models, a difference between the results from the two models may be more difficult to spot. Moreover, in this multi-parameter context, convergence is sometimes compromised, particularly in the large-dependence scenario. In the distribution of the pairwise differences, neither for the transmission parameters nor for the newly estimated severity parameters, can a large difference be seen (figures reported in the Supplementary Information).

For the large dependence scenario, the only notable difference can be seen in the distribution of  ${}^H\theta^{IC}$ : the parameter that links the two datasets, since it defines the probability of IC admission conditional on hospitalization. When the two datasets are jointly analysed, they both contribute to the estimation of  ${}^H\theta^{IC}$ , with hospital data informing the Binomial size in Equation 10 and IC data informing the proportion of people in the more-severe state. When the two datasets are considered independently, the hospital data do not play any role in the inference of  ${}^H\theta^{IC}$ . The proportions of pairwise differences less than or equal to 0 confirm this: the variance of the posterior sample of the parameter  ${}^H\theta^{IC}$  is always lower when inference

is drawn with the approximation to the joint dependent likelihood compared to when the misspecified independent model is adopted (Table 3).

TABLE 3

*Proportion of datasets in which the pairwise difference of variance is smaller or equal to 0 for the transmission and severity parameters.*

Parameter	Proportion of $\text{PWD}(\text{Var}) \leq 0$	
	Small dependence	Large dependence
$\beta$	0.498	0.554
$\pi$	0.464	0.546
$\iota$	0.348	0.202
${}^0\theta^H$	0.466	0.566
${}^H\theta^{IC}$	0.778	1

**4.2.3. Influential parameters.** As a final comparison, a further investigation into the main cause of the difference is undertaken. Starting from the small-dependence scenario, one at a time, each parameter of Table 1 is allowed to take the larger value in simulating the 500 datasets.

Estimates of the five parameters are then obtained according to the misspecified independent and the joint dependent model. The posterior distributions and the plots of the precision statistics are reported in the Supplementary Information. While a detectable difference in the results is observed when all the parameters affecting the level of dependence vary, the same cannot be said when each parameter increases alone. Differences are less evident, with the probability of detection in IC being the most influential parameter, as shown in Table 4, where each column corresponds to a scenario where all the parameters but the header of the column are assumed small.

TABLE 4

*Proportion of datasets in which the pairwise difference of variance is smaller or equal to 0 for the transmission and severity parameters in the scenario with small dependence except for the respective column-name parameter.*

Increased Parameter	${}^0\theta^H$	${}^H\theta^{IC}$	$\zeta^H$	$\zeta^{IC}$
	Parameter	Proportion of $\text{PWD}(\text{Var}) \leq 0$		
$\beta$	0.468	0.454	0.296	0.490
$\pi$	0.450	0.454	0.214	0.496
$\iota$	0.342	0.082	0.052	0.032
${}^0\theta^H$	0.476	0.458	0.290	0.464
${}^H\theta^{IC}$	0.682	0.940	0.072	0.994

**5. Case-study: influenza during the 2017/18 season.** The UK Health Security Agency (UKHSA), formerly Public Health England (PHE), routinely collects several sources of data to monitor influenza cases. Many of these datasets have been used separately to provide information on the transmission (Birrell et al. (2011), Baguelin et al. (2013), Corbella et al. (2018)) and severity (Presanis et al., 2014) of influenza; nevertheless, a joint analysis of all the sources has never been performed. Here a joint model is fitted to multiple data from the 2017/18 influenza season, with the aim of retrospectively characterising both severity and transmission, while appropriately attributing stochasticity to the various processes. Among other datasets, the USISS is analysed and the methodology proposed in Section 3 is used to jointly exploit hospitalisation and IC unit admissions data.

5.1. *Data.* The following datasets are included in the analysis:

- Confirmed influenza cases collected from week 40 of 2017 to week 20 of 2018 via the USISS comprising the weekly count of *IC admissions* from, in principle, all trusts in England (Health Protection Agency, 2011a) and the weekly count of *hospitalizations* at all levels of care in a stratified sentinel sample of the trusts (Health Protection Agency, 2011b);
- Daily counts of *General Practitioners (GPs) consultations* for influenza-like illness (ILI) from a sample of GP monitored by EMIS (Harcourt et al., 2012) or The Phoenix Partnership (The Phoenix Partnership, 2013);
- Observed proportion of respiratory swabs taken on a selected subset of GP patients consulting for ILI that test positive for influenza (*virological positivity*, Health Protection Agency (2014)).
- Results from cross-sectional *serological* surveys that inform on the presence of antibodies in the population (Charlett, 2018).

5.2. *Model Specification.* Figure 5 provides an illustration of the data-generating processes which includes spread of the virus (transmission), probability of mild symptoms and severe outcomes (severity), background ILI cases and detection.

The model is specified in discrete time; intervals of length 1 day are denoted by the index  $u = 1, 2, \dots$ , while 1-week intervals are indexed by  $t = 1, 2, \dots$  (e.g. daily GP consultations are denoted by  $y_u^G$ , while weekly hospitalizations are denoted by  $y_t^H$ ). The remaining notation is similar to that of Section 4, with, e.g.,  ${}_r^J X_s^K$  being the number of people that experienced event  $J$  at time  $r$  and subsequently event  $K$  at time  $s$ . Some essential elements of the model are outlined here; the complete description of the model and the derivations of the data-distributions are provided in the Supplementary Information.

5.2.1. *Transmission and first severity layer.* Denote by  $\xi_u^0$  the number of new infections generated during day  $u$ . A deterministic *SEIR* transmission model, is assumed so that  $\xi_u^0$  is a function of the parameters  $\pi, \iota, \beta, \sigma, \gamma, \kappa$ , representing the proportion of individuals initially immune; the proportion of initially infected/infectious individuals; the transmission rate; the rate of becoming infectious; the recovery rate; and the school-closure effect, respectively.

The infection processes of individuals who will experience hospital admissions,  ${}_u^0 X^H$ , and influenza-related GP consultations,  ${}_u^0 X^F$ , are assumed to follow a time non-homogeneous Poisson process, i.e.:

$$(13) \quad \begin{aligned} \left( {}_u^0 X^H \middle| \xi_u^0, {}^0 \theta^H \right) &\sim \text{Pois} ({}^0 \theta^H \cdot \xi_u^0) & \text{for } u = 0, 1, \dots, U \\ \left( {}_u^0 X^F \middle| \xi_u^0, {}^0 \theta^F \right) &\sim \text{Pois} ({}^0 \theta^F \cdot \xi_u^0) & \text{for } u = 0, 1, \dots, U \end{aligned}$$

with  ${}^0 \theta^F$  and  ${}^0 \theta^H$  denoting the probability of being visited by a GP and being admitted to hospital, respectively.

5.2.2. *GP-consultations.* The inhomogeneous Poisson process of the people who will become mildly symptomatic and consult a GP,  ${}_u^0 X^F$  in Equation 13, is the main component of the likelihood of the GP consultations data. This process too is affected by delays that can be modelled by a discrete r.v. modelling the days elapsing between infection and consulting a practice.

In addition to these individuals, background, non-influenza cases appear in GP consultation data; these endemic cases of other respiratory viruses and bacterial infections often

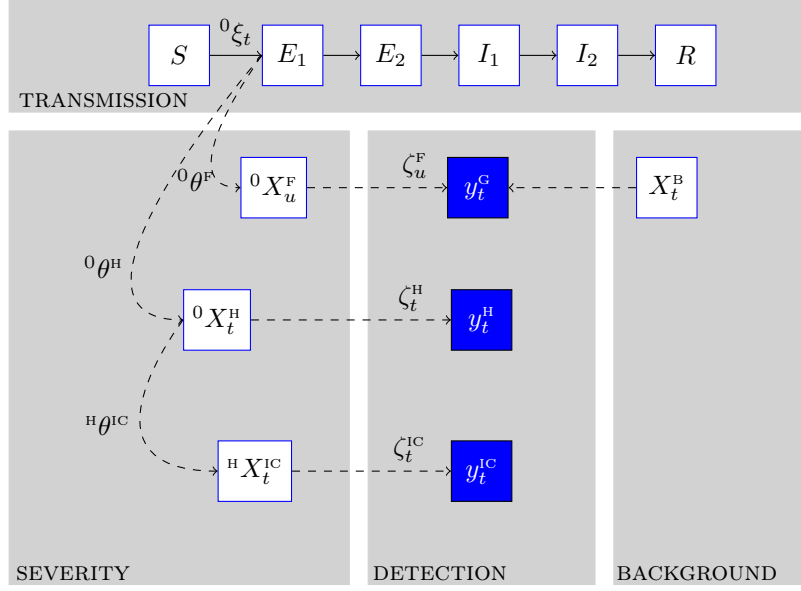


Fig 5: The transmission model classifies the population into susceptible ( $S$ ), exposed ( $E_1, E_2$ ), infectious ( $I_1, I_2$ ) and removed ( $R$ ). The severity model defines the occurrence of: mild flu cases  ${}^0 X^F$  with probability  ${}^0 \theta^F$ , hospital cases  ${}^0 X^H$  with probability  ${}^0 \theta^H$ , and of IC cases conditional on hospitalization  ${}^H X^{IC}$  with probability  ${}^H \theta^{IC}$ . The detection process links cases to data defining the probability of reporting GP consultations ( $\zeta_u^G$ ), hospitalizations ( $\zeta_t^H$ ) and IC admissions ( $\zeta_t^{IC}$ ), respectively. The background process models the non-influenza ILI cases,  $X_t^B$ .

follow a yearly seasonality, peaking around the same time as the seasonal influenza epidemic (Paul, Held and Toschke, 2008). The background seasonality pattern is modelled by a weekly-varying sine-cosine oscillation, similar to Held, Höhle and Hofmann (2005).

The general process describing the number of people consulting a GP with ILI symptoms is then obtained by adding the endemic and epidemic processes. Virological data are used to disentangle the proportion of the former process out of the total.

Lastly, a Binomial emission is again chosen to model the observational process. However, the probability of attending a GP practice is subject to weekly fluctuations, caused by the weekend closure of GP practices, hence a day-of the week distortion effect is included in the probability of detecting a GP consultation.

**5.2.3. Hospitalization and IC admissions.** A model for dependent data on hospitalizations and IC-admissions data is illustrated in Section 3. Here too the joint likelihood is factorised in the marginal distribution of the IC admissions  $Y_{1:T}^{IC}$ , from the Poisson distribution of Equation 11, and the distribution of the hospitalizations  $Y_{1:T}^H$  conditionally on IC data approximated via MC integration as proposed in Algorithm 1.

**5.3. Results.** The joint distribution of the unknown parameter vector (including transmission, severity, background and detection parameters) is derived via GIMH. Weakly-informative priors are assumed for most of the parameters of interest, all the prior distributions used and the estimated posteriors are reported in the Supplementary Information.

The model presents a fair fit to the data (Figure 6) with all the observations being included in the 95% CrIs of the posterior predictive distributions of the GP consultation, virology and hospitalization data. The model, however, struggles to fit IC data which might be in conflict with other sources of information in the model. These data, unlike GP and hospital data, don't suggest a second peak in infection in the latest weeks of winter.

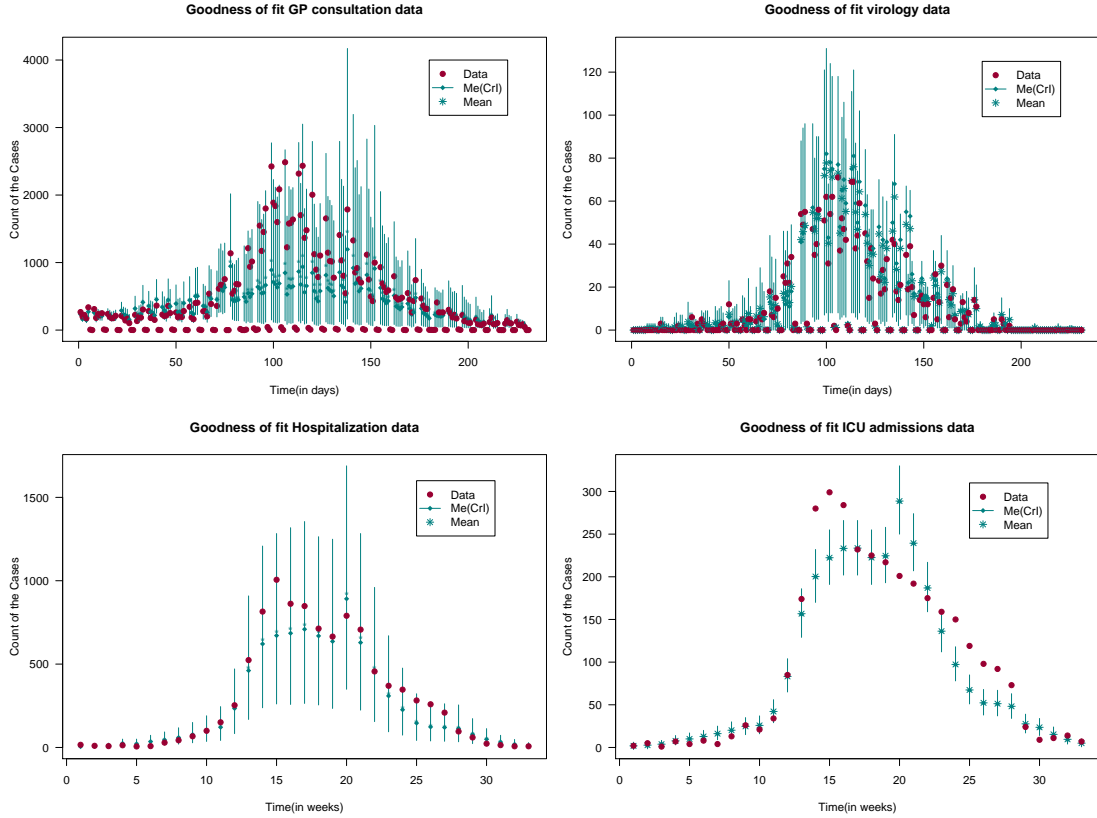
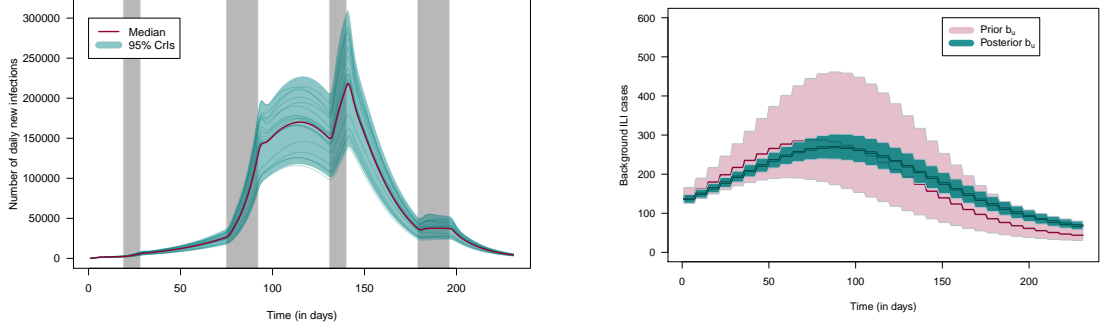


Fig 6: Median and 95% CrIs (green) for the posterior predicted distribution of: GP data (a); virological data (b); hospitalizations (c) and IC admissions (d). Red points are the observed data.

The model provides a comprehensive picture of influenza season 2017/18. Transmission, in terms of daily number of new infections is inferred and background ILI cases are also described (Figure 7). Moreover, all the key severity parameters of interest are well identified and informed by the joint use of the data, including the case-hospitalization risk (Median 0.0032, 95% CrI 0.0022-0.0049) and the hospital-IC admission risk (Median 0.0667, 95% CrI 0.0574-0.078).

The model in all presents many levels of sophistication. Firstly, ILI cases attributable to influenza are disentangled from the background ILI, which, while not being directly related to influenza, contributes to pressure on GP practices. Secondly, the model accounts for peculiarities of the GP data, such as the day-of-the-week variation, uncovering the true underlying transmission and severity process. Lastly and more importantly, exact inference from dependent data via MC methods enables the simultaneous use of information from hospital and IC surveillance.



(a) Median (red) and 95% CrIs (green) of the daily number of new infections. The grey areas corresponding to periods of lower-transmission (school holidays). 20 randomly selected trajectories are also plotted as thin green lines.

(b) Median (solid line) and 95% CrIs (shaded area) of the prior (red) and posterior (green) for  $b_u$ , the mean of the rate of the daily number of non-influenza ILI GP consultations.

Fig 7: Posterior results from the joint analysis of 2017/18 data: transmission and background.

**6. Discussion.** This work contributes to the state-of-the-art literature on the analysis of epidemic data, from a methodological/computational perspective, providing new tools, applicable to a wide class of problems that includes dependent data; and from an application perspective, providing innovative results on the analysis of influenza from multiple sources.

**6.1. Methodological and computational perspective.** Section 2 contains a concise review of SSMs and their analysis, particularly focussed on the analysis of multiple epidemic data. There are other reviews of these methods in the literature (Kantas et al. (2015); Schön et al. (2018)), some of which even target epidemic applications (McKinley et al. (2014); Dureau, Ballesteros and Bogich (2013); Ionides, Bretó and King (2006)). However, these reviews mainly address temporal dependences and, to the knowledge of the authors, little is known about the dependence across other domains. In the context of epidemic analysis, where temporal dependence can be easily overcome through realistic deterministic approximations of transmission dynamics, it is key to consider the sources of stochasticity and dependence linked to other processes (in this case the severity process) and its implications.

Sections 3 and 4 embrace this challenge and highlight the possible complexities of such an analysis. Starting from a specific example, where there is dependence between data sources, an approach to the estimation of the static parameters of the system is proposed. Key aspects such as overlaps between datasets and delays between consecutive events are then revealed to affect results. It is shown via simulation that simplifying assumptions, which assume independence among data and avoid expensive integration, lead to overconfident results and misleadingly narrow interval estimates.

Our general and comprehensive way to set up epidemic models are paired with a specific estimation routine for their static parameters: pseudo-marginal methods. These methods are robust and simple to set up since they rely on the standard MH algorithms, however they are expensive in two respects: firstly, a high number of simulations of the hidden states is required at each iteration of the static parameter to approximate its likelihood; and, secondly, the parameter space might be explored inefficiently due to their random walk behaviour. The first of these aspects might be addressed, for example, by converting to a data-augmented (DA) MCMC perspective (O'Neill and Roberts, 1999), which only needs a single sample from the hidden states per MCMC iteration. DA approaches however, require tailored implementations for each different system considered, and therefore do not provide a general recipe applicable

to a wide class of models. In terms of exploration of the parameter space, the unavailability of closed-form likelihood prevents the use of popular gradient based methods (e.g. Hamiltonian Monte Carlo (HMC) (Neal et al., 2011) or the more recent Piecewise Deterministic Markov Process (PDMP) sampler (Bierkens, Fearnhead and Roberts, 2019)). Alternatively, a natural way to improve the estimation routine would be to consider sequential Monte Carlo (SMC) methods on the parameter space, which in this context can be thought of as SMC<sup>2</sup> (Chopin, Jacob and Papaspiliopoulos, 2013).

**6.2. Application perspective.** The ability of estimating key transmission and severity parameters from epidemic data has never been more crucial. With the COVID-19 epidemic affecting almost every aspect of people's life, evidence-based decision-making has become an imperative aspect of public health policy. Uncertainty quantification around central estimates is key to understand both the extreme possible scenarios that could present in the near future and what further information is needed to increase knowledge and inform decisions.

Section 5 of the paper proposes a complex joint analysis of multiple data on influenza where both mild and severe cases inform transmission and severity parameters. The model presents multiple levels of sophistication including: the use of dependent data; the use of data from both non-confirmed and confirmed cases; the disentangling of background ILI cases; the presence of delays between events. The key innovation of this model is that it matches a deterministic transmission dynamic with a stochastic severity and reporting process. In this sense it differentiates from other works that make joint use of multiple data but assume deterministic severity dynamics (e.g. Keeling et al. (2020)).

Shubin et al. (2016) proposes a similar analysis of the 2009 pandemic in Finland. Even though his model presents many interesting aspects (e.g. the inclusion of both environmental and demographic stochasticity), unrealistic simplifications are made to allow for estimation in reasonable time, including the exclusion of an *exposed* compartment, the discretization of time into extremely-large intervals (one week), and the assumption of no time elapsing between events of increasing severity. We consider our approach as a valid alternative to Shubin et al. (2016), especially on a large population such as that of England, where the deterministic assumption is even more likely to hold.

Going forward, the model could be extended in, at least, two interesting ways: firstly, population heterogeneity could be considered, through the formulation of an age-specific model that makes use of contact patterns between age groups; and secondly, more overdispersion could be allowed in the severity process by, for example, replacing Poisson r.v.s with Negative Binomial r.v.s. These changes would almost certainly improve the fitting of the model to data.

Lastly, other interesting analyses could be performed starting from the proposed model. The analysis presented here is retrospective and aimed at a posterior estimation of key epidemiological parameters; it would be interesting to test the predictive ability of such a model so that it can be used in real time for decision-making on resource allocation for different healthcare facilities. Moreover, more insights could be gained from the quantification of the contribution to inference provided by each separate dataset from a value of information perspective Jackson et al. (2019).

**Acknowledgements.** The author would like to thank colleagues at Public Health England, particularly Dr Richard Pebody, Dr Andre Charlett and Dr Nikolaos Panagiotopoulos, for providing the data and prior information for the analysis in Section 6. We are grateful to Dr Michail Shubin for insightful discussions on the earlier work on dependent data streams. Lastly, Dr Trevelyan J McKinley and Dr Paul Kirk provided useful feedback on an earlier version of this work for which we are thankful.

AC is supported by Bayes4Health EPSRC Grant EP/R018561/1. All four authors were supported by the MRC, programme grant MC\_UU\_00002/11.

## SUPPLEMENTARY MATERIAL

**Supplementary Information**

This report contains further work on the study of dependence between data and supplementary information to the study of Section 5. The former includes further comments on SSM inference, the derivations of Algorithm 1 and the results from the simulation study of Section 4. The latter includes extensive explanation of the model, inferential methods and results of the analysis.

**Supplementary code and data**

Code for the simulation study in Section 4 and the analysis of Section 5 are available at <https://github.com/alicecorbella/EpiDependentData>. The data analysed in Section 5 are based on routine health-care data, which cannot be made available to others by the study authors. Requests to access these non-publicly available data are handled by the [Public Health England Office for Data Release](#) and its successor at the [UK Health Security Agency](#).

## REFERENCES

HEALTH PROTECTION AGENCY (2011a). Sources of UK flu data—Influenza Surveillance in the United Kingdom. Available at the following [link](#).

HEALTH PROTECTION AGENCY (2011b). UK Severe Influenza Surveillance System (USISS) - Protocol for sentinel Acute NHS Trusts 2011-12. Available at the following [link](#).

HEALTH PROTECTION AGENCY (2014). Sources of UK Flu Data: Influenza Surveillance in the United Kingdom. Available at the following [link](#).

ANDERSON, J. L. (1996). A method for producing and evaluating probabilistic forecasts from ensemble model integrations. *Journal of climate* **9** 1518–1530. DOI: [10.1175/1520-0442\(1996\)009](https://doi.org/10.1175/1520-0442(1996)009).

ANDERSSON, H. and BRITTON, T. (2012). *Stochastic epidemic models and their statistical analysis* **151**. Springer Science & Business Media.

ANDRIEU, C., DOUCET, A. and HOLENSTEIN, R. (2010). Particle markov chain monte carlo methods. *Journal of the Royal Statistical Society: Series B (Statistical Methodology)* **72** 269–342.

ANDRIEU, C. and ROBERTS, G. O. (2009). The pseudo-marginal approach for efficient Monte Carlo computations. *The Annals of Statistics* **37** 697–725. DOI: [10.1214/07-AOS574](https://doi.org/10.1214/07-AOS574).

ARULAMPALAM, M. S., MASKELL, S., GORDON, N. and CLAPP, T. (2002). A tutorial on particle filters for online nonlinear/non-Gaussian Bayesian tracking. *IEEE Transactions on signal processing* **50** 174–188. DOI: [10.1109/78.978374](https://doi.org/10.1109/78.978374).

BAGUELIN, M., FLASCHE, S., CAMACHO, A., DEMIRIS, N., MILLER, E. and EDMUNDS, W. J. (2013). Assessing optimal target populations for influenza vaccination programmes: an evidence synthesis and modelling study. *PLoS medicine* **10** e1001527.

BEAUMONT, M. A. (2003). Estimation of population growth or decline in genetically monitored populations. *Genetics* **164** 1139–1160.

BIERKENS, J., FEARNHEAD, P. and ROBERTS, G. (2019). The zig-zag process and super-efficient sampling for Bayesian analysis of big data. *The Annals of Statistics* **47** 1288–1320.

BIRRELL, P. J., DE ANGELIS, D. and PRESANIS, A. M. (2018). Evidence synthesis for stochastic epidemic models. *Statistical science: a review journal of the Institute of Mathematical Statistics* **33** 34. DOI: [10.1214%2F17-STS631](https://doi.org/10.1214%2F17-STS631).

BIRRELL, P. J., KETSETZIS, G., GAY, N. J., COOPER, B. S., PRESANIS, A. M., HARRIS, R. J., CHARLETT, A., ZHANG, X.-S., WHITE, P. J., PEBODY, R. G. et al. (2011). Bayesian modeling to unmask and predict influenza A/H1N1pdm dynamics in London. *Proceedings of the National Academy of Sciences* **108** 18238–18243. DOI: [10.1073/pnas.1103002108](https://doi.org/10.1073/pnas.1103002108).

BIRRELL, P., BLAKE, J., VAN LEEUWEN, E., GENT, N. and DE ANGELIS, D. (2021). Real-time nowcasting and forecasting of COVID-19 dynamics in England: the first wave. *Philosophical Transactions of the Royal Society B* **376** 20200279. DOI: [10.1098/rstb.2020.0279](https://doi.org/10.1098/rstb.2020.0279).

BODDINGTON, N., VERLANDER, N. and PEBODY, R. (2017). Developing a system to estimate the severity of influenza infection in England: findings from a hospital-based surveillance system between 2010/2011 and 2014/2015. *Epidemiology & Infection* **145** 1461–1470.

BRETÓ, C., HE, D., IONIDES, E. L. and KING, A. A. (2009). Time series analysis via mechanistic models. *The Annals of Applied Statistics* 319–348.

BRITTON, T. (2010). Stochastic epidemic models: a survey. *Mathematical biosciences* **225** 24–35.

BROCKWELL, P. J., BROCKWELL, P. J., DAVIS, R. A. and DAVIS, R. A. (2016). *Introduction to time series and forecasting*. Springer.

BROOKMEYER, R., GAIL, M. H., GAIL, M. H. et al. (1994). *AIDS epidemiology: a quantitative approach*. Oxford University Press on Demand.

BROOKS, S., GELMAN, A., JONES, G. and MENG, X.-L. (2011). *Handbook of markov chain monte carlo*. CRC press.

CHARLETT, A. (2018). Personal communication on the level of immunity priori 2017/18 Influenza season.

CHOPIN, N., JACOB, P. E. and PAPASILIOPOULOS, O. (2013). SMC2: an efficient algorithm for sequential analysis of state space models. *Journal of the Royal Statistical Society: Series B (Statistical Methodology)* **75** 397–426.

CHURCHILL, G. A. (2005). Hidden M arkov Models. *Encyclopedia of Biostatistics* **4**.

CORBELLA, A. (2019). Statistical inference in stochastic/deterministic epidemic models to jointly estimate transmission and severity, PhD thesis, University of Cambridge DOI: [10.17863/CAM.41539](https://doi.org/10.17863/CAM.41539).

CORBELLA, A., ZHANG, X.-S., BIRRELL, P. J., BODDINGTON, N., PEBODY, R. G., PRESANIS, A. M. and DE ANGELIS, D. (2018). Exploiting routinely collected severe case data to monitor and predict influenza outbreaks. *BMC public health* **18** 1–11.

DIEKMANN, O., HEESTERBEEK, H. and BRITTON, T. (2012). *Mathematical tools for understanding infectious disease dynamics*. Princeton University Press.

DUKIC, V., LOPES, H. F. and POLSON, N. G. (2012). Tracking epidemics with Google flu trends data and a state-space SER model. *Journal of the American Statistical Association* **107** 1410–1426.

DUREAU, J., BALLESTEROS, S. and BOGICH, T. (2013). SSM: Inference for time series analysis with State Space Models. *arXiv preprint arXiv:1307.5626*.

FUNK, S., CAMACHO, A., KUCHARSKI, A. J., EGGO, R. M. and EDMUNDS, W. J. (2018). Real-time forecasting of infectious disease dynamics with a stochastic semi-mechanistic model. *Epidemics* **22** 56–61. DOI: [10.1016/j.epidem.2016.11.003](https://doi.org/10.1016/j.epidem.2016.11.003).

HARCOURT, S., SMITH, G., ELLIOT, A., PEBODY, R., CHARLETT, A., IBBOTSON, S., REGAN, M. and HIPPISLEY-COX, J. (2012). Use of a large general practice syndromic surveillance system to monitor the progress of the influenza A (H1N1) pandemic 2009 in the UK. *Epidemiology & Infection* **140** 100–105.

HASTINGS, W. K. (1970). Monte Carlo sampling methods using Markov chains and their applications.

HELD, L., HÖHLE, M. and HOFMANN, M. (2005). A statistical framework for the analysis of multivariate infectious disease surveillance counts. *Statistical modelling* **5** 187–199.

IONIDES, E. L., BRETÓ, C. and KING, A. A. (2006). Inference for nonlinear dynamical systems. *Proceedings of the National Academy of Sciences* **103** 18438–18443.

JACKSON, C., PRESANIS, A., CONTI, S. and DE ANGELIS, D. (2019). Value of information: Sensitivity analysis and research design in Bayesian evidence synthesis. *Journal of the American Statistical Association*. DOI: [10.1080/01621459.2018.1562932](https://doi.org/10.1080/01621459.2018.1562932).

KALMAN, R. E. (1960). A new approach to linear filtering and prediction problems.

KANTAS, N., DOUCET, A., SINGH, S. S., MACIEJOWSKI, J. and CHOPIN, N. (2015). On particle methods for parameter estimation in state-space models. *Statistical science* **30** 328–351.

KEELING, M. J. and ROHANI, P. (2011). *Modeling infectious diseases in humans and animals*. Princeton university press.

KEELING, M. J., DYSON, L., GUYVER-FLETCHER, G., HOLMES, A., SEMPLE, M. G., INVESTIGATORS, I., TILDESLEY, M. J. and HILL, E. M. (2020). Fitting to the UK COVID-19 outbreak, short-term forecasts and estimating the reproductive number. *Statistical Methods in Medical Research*. DOI: [10.1101/2020.08.04.20163782](https://doi.org/10.1101/2020.08.04.20163782).

KERMACK, W. O. and MCKENDRICK, A. G. (1927). A contribution to the mathematical theory of epidemics. *Proceedings of the royal society of london. Series A, Containing papers of a mathematical and physical character* **115** 700–721.

KING, A. A., NGUYEN, D. and IONIDES, E. L. (2015). Statistical inference for partially observed Markov processes via the R package pomp. *arXiv preprint arXiv:1509.00503*.

KINGMAN, J. F. C. (1992). *Poisson processes* **3**. Clarendon Press.

LEKONE, P. E. and FINKENSTÄDT, B. F. (2006). Statistical inference in a stochastic epidemic SEIR model with control intervention: Ebola as a case study. *Biometrics* **62** 1170–1177. DOI: [10.1111/j.1541-0420.2006.00609.x](https://doi.org/10.1111/j.1541-0420.2006.00609.x).

LINDSTEN, F. and SCHÖN, T. B. (2013). Backward simulation methods for Monte Carlo statistical inference. *Foundations and Trends® in Machine Learning* **6** 1–143.

LINDSTEN, F. and SCHÖN, T. B. (2017). Learning of dynamical systems. Particle filters and Markov chain methods.

MAGPANTAY, F., DE CELLES, M. D., ROHANI, P. and KING, A. (2016). Pertussis immunity and epidemiology: mode and duration of vaccine-induced immunity. *Parasitology* **143** 835–849.

MCKINLEY, T. J., ROSS, J. V., DEARDON, R. and COOK, A. R. (2014). Simulation-based Bayesian inference for epidemic models. *Computational Statistics & Data Analysis* **71** 434–447.

METROPOLIS, N., ROSENBLUTH, A. W., ROSENBLUTH, M. N., TELLER, A. H. and TELLER, E. (1953). Equation of state calculations by fast computing machines. *The journal of chemical physics* **21** 1087–1092.

NEAL, R. M. et al. (2011). MCMC using Hamiltonian dynamics. *Handbook of markov chain monte carlo* **2** 2.

NISHIURA, H. (2011). Real-time forecasting of an epidemic using a discrete time stochastic model: a case study of pandemic influenza (H1N1-2009). *Biomedical engineering online* **10** 1–16. DOI: [0.1186/1475-925X-10-15](https://doi.org/10.1186/1475-925X-10-15).

O'NEILL, P. D. and ROBERTS, G. O. (1999). Bayesian inference for partially observed stochastic epidemics. *Journal of the Royal Statistical Society: Series A (Statistics in Society)* **162** 121–129.

THE PHOENIX PARTNERSHIP (2013). Real-time Syndromic Surveillance.

PAUL, M., HELD, L. and TOSCHKE, A. M. (2008). Multivariate modelling of infectious disease surveillance data. *Statistics in medicine* **27** 6250–6267.

PRESANIS, A. M., DE ANGELIS, D., NEW YORK CITY SWINE FLU INVESTIGATION TEAM, HAGY, A., REED, C., RILEY, S., COOPER, B. S., FINELLI, L., BIEDRZYCKI, P. and LIPSITCH, M. (2009). The severity of pandemic H1N1 influenza in the United States, from April to July 2009: a Bayesian analysis. *PLoS medicine* **6** e1000207.

PRESANIS, A. M., OHLSSEN, D., SPIEGELHALTER, D. J. and DE ANGELIS, D. (2013). Conflict diagnostics in directed acyclic graphs, with applications in Bayesian evidence synthesis. *Statistical Science* **28** 376–397. DOI: [10.1214/13-STS426](https://doi.org/10.1214/13-STS426).

PRESANIS, A. M., PEBODY, R. G., BIRRELL, P. J., TOM, B. D., GREEN, H. K., DURNALL, H., FLEMING, D. and DE ANGELIS, D. (2014). Synthesising evidence to estimate pandemic (2009) A/H1N1 influenza severity in 2009–2011. *The Annals of Applied Statistics* 2378–2403. DOI: [10.1214/14-AOAS775](https://doi.org/10.1214/14-AOAS775).

SCHÖN, T. B., SVENSSON, A., MURRAY, L. and LINDSTEN, F. (2018). Probabilistic learning of nonlinear dynamical systems using sequential Monte Carlo. *Mechanical systems and signal processing* **104** 866–883. DOI: [10.1016/j.ymssp.2017.10.033](https://doi.org/10.1016/j.ymssp.2017.10.033).

SHUBIN, M., LEBEDEV, A., LYYTIKÄINEN, O. and AURANEN, K. (2016). Revealing the true incidence of pandemic A (H1N1) pdm09 influenza in Finland during the first two seasons—An analysis based on a dynamic transmission model. *PLoS computational biology* **12** e1004803.

SOLIN, A., KOK, M., WAHLSTRÖM, N., SCHÖN, T. B. and SÄRKKÄ, S. (2018). Modeling and interpolation of the ambient magnetic field by Gaussian processes. *IEEE Transactions on robotics* **34** 1112–1127. DOI: [10.1109/TRO.2018.2830326](https://doi.org/10.1109/TRO.2018.2830326).

UK HEALTH SECURITY AGENCY (UKHSA) (2021). Sources of UK flu data—Influenza Surveillance in the United Kingdom. Available at the following [link](#).

WEIDEMANN, F., DEHNERT, M., KOCH, J., WICHMANN, O. and HÖHLE, M. (2014). Bayesian parameter inference for dynamic infectious disease modelling: rotavirus in Germany. *Statistics in Medicine* **33** 1580–1599. DOI: [10.1002/sim.6041](https://doi.org/10.1002/sim.6041).